RSC Advances

Gold Nanospirals

Journal:	*RSC Advances*
Manuscript ID:	RA-ART-06-2015-011492.R1
Article Type:	Paper
Date Submitted by the Author:	26-Aug-2015

Complete List of Authors:	Chang, Yu-Hsu; National Taipei University of Technology, Wu, Yu-Chuan; National Taipei University of Technology, Hsu, Ya-Ting; National Taipei University of Technology, Huang, Shih-Hao; National Taipei University of Technology, Huang, Yi-Chin; National Taipei University of Technology, Chiu, Hsin-Tien; National Chiao Tung University,

Journal Name

ARTICLE

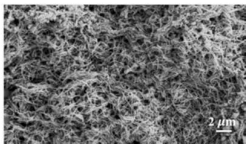

Received 00th January 20xx,
Accepted 00th January 20xx

DOI: 10.1039/x0xx00000x

www.rsc.org/

Gold Nanospirals

Yu-Hsu Chang,*[a] Yu-Chuan Wu,[a] Ya-Ting Hsu,[a] Shih-Hao Huang,[a] Yi-Chin Huang[a] and Hsin-Tien Chiu[b]

This study used galvanic displacement reaction for aluminum-gold oxidation-reduction and added surfactants to act as capping agents to control the morphology and size of gold growth. Three surfactants, namely cetyltrimethylammonium bromide, polyvinylpyrrolidone, and poly(ethylene glycol)(12) tridecyl ether, were added to $HAuCl_4$ (aq) to create novel gold nanospirals (AuNSs) 200-500 nm in diameter and tens of μm in length. Transmission electron microscopy analysis showed that the AuNSs were face-centered cubic in structure and that growths on the {111} facet were growth twins with mirror symmetry. Used as the base material for surface-enhanced Raman scattering, the structure of the trunk and dendrimers of the AuNSs create numerous hot spots, exhibiting a superior surface enhancement effect.

1. Introduction

In recent years, it has been found that matter on a nanoscale has unique characteristics not held by traditional materials; precious metal nanostructures in particular catalytic,[1] surface-enhanced Raman scattering (SERS),[2,3] and light,[4,5] electrical,[6] and biological sensing qualities[7] of great interest to the scientific community. Differences in appearance and size also affect the physical properties of noble metal nanomaterials. Past literature has noted that certain nanomaterials with special appearances can be controlled in an artificial environment. For example, the unique atomic structures of ultrafine gold nanowires,[8] thin tellurium nanobelts and nanotubes,[9] icosahedral Ag-Au nanowires,[10] double helix Au-Ag nanowires,[11] helical PbSe nanowires,[12] and ZnO nanohelices[13] are vastly different from traditional bulk materials. Surfactants are added to many nanomaterial synthesis reactions to control the size and shape of the product. Surfactants provide two functions in a reaction that influence the growth mechanism of products.[14] The first is using the micelles created by the surfactants in solution as a soft template in which the metal ions can carry out reduction reactions. The metal atoms slowly accumulate inside the micelle to create a one-dimensional metallic substance. The second is using surfactants as a crystal growth capping agent. The surfactant is adsorbed by certain metallic crystal facets, forcing crystal growth to follow a specific path in order to create a one-dimensional structure. This study used aluminum (E^0=1.66V) and gold (E^0=1.42V) as their reducing potential difference produces spontaneous galvanic displacement reactions to create gold nanospirals (AuNSs). To obtain one-dimensional nanostructures, a confined space must be provided for anisotropic growth; therefore, surfactants were added to act as the capping agents to control the structure of the product. Three surfactants, cetyltrimethylammonium bromide (CTAB), polyvinylpyrrolidone (PVP), and poly(ethylene glycol)(12) tridecyl ether (PEG) were added to the reaction to aid the Au^{3+} ions reduce into numerous one-dimensional gold arrays, a metallic nanostructure with a unique morphology, on an aluminum surface. To our knowledge, this is the first report of the synthesis of gold nanowires with a helical structure in a one-pot reaction.

2. Experimental

2.1 Synthesis of AuNSs

First, the Al foil (thickness 0.25 mm, 99.999%, Sigma-Aldrich) was cut into 0.5*0.5 cm^2 pieces. The surfactants were added to 20 mL of 1.5 mM $HAuCl_4$(aq) (gold (III) chloride trihydrate, 99.9%, Aldrich) aqueous solution such that the concentration of PEG ($C_{13}H_{27}(OCH_2CH_2)_nOH$, n~12, Aldrich) was 1 mM, the concentration of PVP ($(C_6H_9NO)_n$, MW~55000, Aldrich) was 0.5 mM, and the concentration of CTAB ($CH_3(CH_2)_{15}N(CH_3)_3Br$, Sigma) was 2 mM. Next, the prepared pieces of Al foil were placed in the solution at 21°C. After 20 h, deionized water was added to terminate the reactions. Samples were extracted and blown dry with nitrogen gas.

2.2 Characterizations and Spectroscopic Measurements

Examinations of the morphology of the samples were carried out with a scanning electron microscope (Hitachi S-4700) equipped with an energy-dispersive X-ray spectrometer (EDS).

[a] Department of Materials and Mineral Resources Engineering/Institute of Mineral Resources Engineering, National Taipei University of Technology, Taipei 10608, Taiwan R.O.C.
[b] Department of Applied Chemistry, National Chiao Tung University, Hsinchu 300, Taiwan R.O.C.

† Footnotes relating to the title and/or authors should appear here. Electronic Supplementary Information (ESI) available: [details of any supplementary information available should be included here]. See DOI: 10.1039/x0xx00000x

The transmission electron microscopy (TEM) images and electron diffraction patterns were obtained using a transmission electron microscope (JEOL 2100F). The SERS and mapping images were acquired from a Raman spectrometer (NTEGA NT-MDT) using a 632.8 nm He-Ne laser (power ~1.5 mW). The laser beam was focused to a spot approximately 1 μm^2 with an accumulation time of 10 s. The collection time for the mapping image was 1 s.

3. Results and discussion

The SEM image in Figure 1a shows spiral structures in high concentration on the aluminum substrate. The nanospiral structure is apparent at high magnification (Fig. 1b). EDS analysis showed that the product was mainly composed of elemental gold. The trunk of the AuNSs has a helical structure and the outer surface is made up of aggregate granule branches. These one-dimensional nanomaterials were 200-500 nm in diameter and tens of µm in length. The trunks of a few of the products were more linear than others, yet still exhibiting a twisting phenomenon. The surface of the AuNSs resembled dendrimers composed of small, layered nanoparticles. Figure 2a shows the SEM image of one AuNS, illustrating that the growth pattern is counter clockwise.

To observe the atom arrangement, a smaller AuNS formed at the beginning of the reaction (Fig. 2b) was selected for high-resolution transmission electron microscopy (HRTEM) and fast Fourier transform (FFT) analysis. The three circled areas (R_1, R_2, and R_3) are three grain boundaries. Three boundaries divided the trunk of the AuNS into four sections (A, B, C, and D) for analysis. In sections A and B_1 (Fig. 2c), the HRTEM image and the corresponding FFT image indicate that the $(\bar{1}1\bar{1})$ and $(1\bar{1}1)$ planes in FFT-A and FFT-B_1, respectively, are vertical to R_1; thus, the twin plane R_1 is the $(\bar{1}1\bar{1})$ crystal plane. The two sides of the twin plane, sections A and B_1, is the $(\bar{1}\bar{1}1)$ plane and the included angle is 141°. In Figure 2d, the HRTEM image shows that the atom arrangement in sections B_2 and C_1 do not have twin plane mirror symmetry, yet FFT-B_2 and FFT-C_1 have the same diffraction points; therefore, it can be confirmed that R_2 is a stacking fault. Stacking faults have crystal defects and are not twin planes. In sections C_2 and D (Figure 2e), the HRTEM image and the corresponding FFT images indicate that the $(\bar{1}\bar{1}1)$ and $(11\bar{1})$ planes in FFT-C_2 and FFT-D, respectively, are vertical to R_3; thus, the twin plane R_3 is corresponding to the $(\bar{1}\bar{1}1)$ crystal plane. The two sides of the crystal plane, sections C_2 and D, reflect the $(\bar{1}1\bar{1})$ plane and the included angle is 141°. The above TEM analysis shows that when AuNSs grow, growth twins with mirror symmetry form at the {111} twin plane. AuNSs form by twinning and are thus growth twins. During growth, as the {111} twin plane has a 70.5° angle difference (the included angle between R_1 and R_3), the gold atoms stack in a spiral to form AuNSs.

With regards to the AuNSs surrounding microstructure analysis, TEM observation clearly shows a dendrimer appearance (Fig. 3a). The cross-sectional TEM sample was prepared by focused ion beam milling. The circled area shows a grain boundary, R4, that was selected for analysis; the sides of R4 are denoted as sections E and F. Converting the HRTEM image for sections E and F to FFT patterns revealed that $(\bar{1}1\bar{1})$ and $(1\bar{1}1)$ of FFT-E and FFT-F , respectively, are vertical to R_4. Therefore, it was deduced that the twin plane was $(\bar{1}1\bar{1})$ and the plane to either side of the twin plane was $(\bar{1}\bar{1}1)$. The included angle between the two planes was 141˚ (Fig. 3c). The above analysis revealed that as the dendrimers on the surface of the AuNSs, they create twin structures with mirror symmetry on the $(\bar{1}\bar{1}1)$ or $(\bar{1}1\bar{1})$ twin plane which creates a spiraling phenomenon. This also explains both the spiral of the AuNS trunk and that the morphology of the products is also dependent on the formation of the dendrimers.

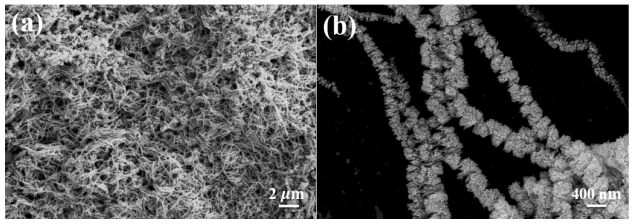

Fig. 1 (a) and (b) are SEM images of AuNSs at low and high magnifications, respectively.

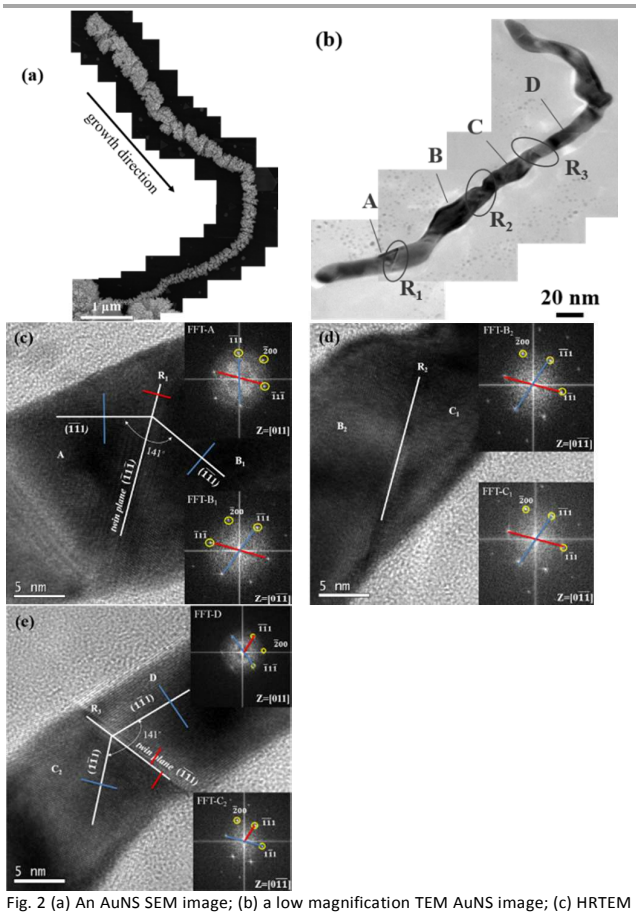

Fig. 2 (a) An AuNS SEM image; (b) a low magnification TEM AuNS image; (c) HRTEM and FFT images near R_1; (d) HRTEM and FFT images near R_2; (e) HRTEM and FFT images near R_3.

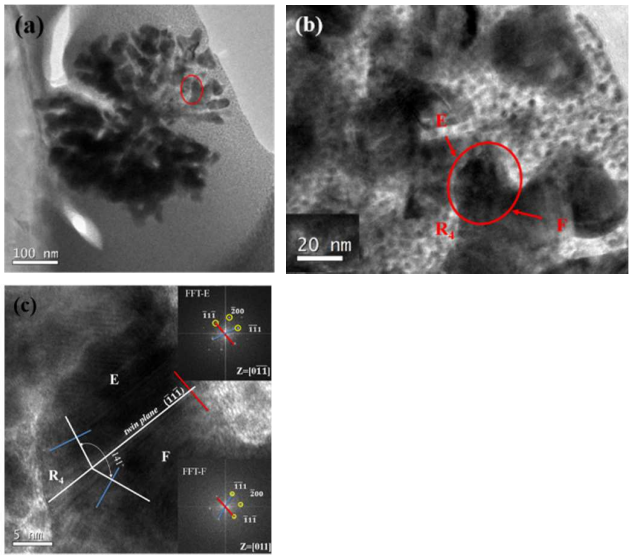

Fig. 3 (a) AuNS cross section low magnification TEM image showing the dendrimer shape; (b) AuNS cross section high magnification TEM image; (c) HRTEM image and the corresponding FFT patterns for R4 in Figure 3b.

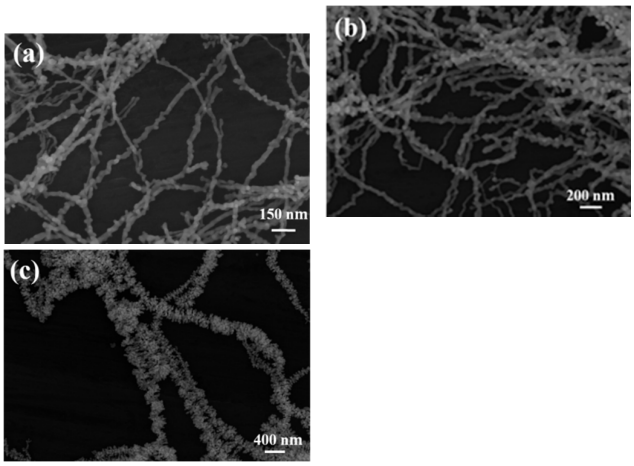

Fig. 4 SEM images of AuNSs at different reaction times: (a) 3 hours, (b) 9 hours, and (c) 18 hours

Samples with a reaction time of 3, 9, and 18 h were observed using an SEM to investigate their appearance and understand the AuNS growth process. The SEM images in Figure 4 show that at a reaction time of 3 h, the AuNSs diameters were less than 50 nm and the trunks had already begun to twist. As a reaction time of 9 h, the AuNSs began to grow branches outward from their helical structures. At 18 h, AuNSs with loose outer dendrimers had begun to form. Therefore, it was speculated that the growth process for these 1D Au nanostructures, as shown in Figure 4, begin with a twisting Au nanowire and later gold dendrimers begin to grow around the nanowire which finally becomes a spiral structure.

When using a seed-mediated, surfactant-directed method to synthesize gold nanomaterials, the surfactant CTAB creates a double layer on the surface of the gold which guides the gold to grow into a one-dimensional nanorod[15-17]. Hydroxyl groups are the functional end groups of PVP which acts as a mild reducing agent and/or a stabilizer or capping agent to prevent powder aggregation[18,19]. The PVP concentration in this study was only 0.5 mM, the slow reduction rate help nucleation and crystal growth be kinetically controlled.[20] PVP is first adsorbed on the nanoseed surface, whereas CTAB first forms a $[AuCl_2^-]$-$[CTA^+]$ complex with gold ions before being adsorbed to the nanoseed surface.[21] The nanoseed facets with high surface energy are {110} and {100}, which promotes a high growth rate due to the Au-CTA catalyzed reduction.[22] On the low-surface-energy facet {111}, PVP adsorption may suppress Au atom stacking. With regards to PEG, molecule dynamic simulation indicated that it would form a helical conformation in water.[23,24] However, the three surfactants undergo reactions at the solid-liquid interface simultaneously, which complicates the overall system. We roughly concluded the influences the three surfactants have on AuNS growth. CTAB creates a double layer structure on the surface of the gold which forces the nanogold to grow in one direction; PVP acts as a capping agent which surrounds the surface of the nanogold; the helical structure of PEG helps the product to grow in a spiral.

4. Applications

Precious metal nanostructures have excellent SERS properties; therefore, SERS measurements were conducted using AuNSs as the substrates and 4-mercaptobenzoic acid (4MBA; 1 mM in ethanolic solution) as a probe. Pure 4MBA powder Raman signals at 1075 cm^{-1} and 1590 cm^{-1} were $_{\nu 12}C$-C_{ring} and $_{\nu 8a}C$-C_{ring}, respectively, where ν=stretch and ring=ring breathing mode.[25] Figure 5a shows the SEM image for a test strip. Figures 5b and 6c show SERS mapping images at 1075 cm^{-1} and 1590 cm^{-1}, respectively. The images clearly show highly concentrated clusters of AuNSs have a superior strengthening effect; SERS intensity reached 11,000-13,000 counts. Where AuNSs were less dense and at the extremities, I_{SERS} intensity was approximately 5,000 counts. These results verify that the AuNSs have an excellent SERS effect. The enhancement may be so significant because where AuNSs are denser and many nanospirals overlap, the outlying dendrimers create numerous hot spots. When the surface plasmon band is restricted to an extremely small area (~2 nm), photoexcitation is enhanced. When the excitation frequency and the resonant frequency of the absorbing molecules are the same, SERS is created, strengthening the signal.[26]

Conclusions

This study used a simple galvanic displacement reaction and added three surfactants, CTAB, PVP, and PEG, to $HAuCl_4$ (aq) to act as capping agents to control appearance and size. Reaction temperature was also adjusted to obtain AuNSs with 200-500 nm in diameter and tens of μm in length on an aluminum substrate. The interaction between the three surfactants played a critical role in the formation of the helical structure. If

PEG or PVP were not added, the reaction temperature was changed, or $HAuCl_4$(aq) or CTAB concentrations were changed, only nanoparticles and dendrimers of inconsistent shape would have formed. With regards to SERS properties, the intensity was 6-19 times greater than that of gold nanoparticles regardless of whether the AuNSs were dense, scattered, or at the extremities, showing a superior

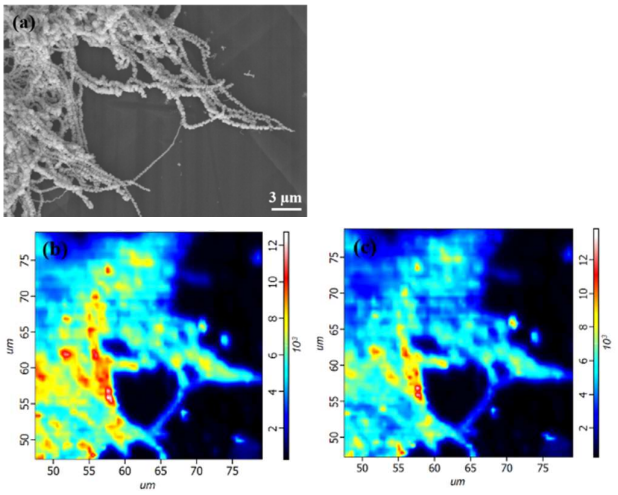

enhancement effect. As the surface of the spiral material is made up of dense Au nanostructures, we used the advantages of this structure to conduct catalytic reactions assisted by surface plasmon resonances.

Fig. 5 AuNSs (a) an SEM image and the correlated Raman microspectroscopic mapping image measured at (b) 1075 cm^{-1} and (c) 1590 cm^{-1}.

Acknowledgements

The authors thank the Ministry of Science and Technology of Taiwan, Republic of China (NSC-99-2113-M-027-003) for financial support.

Notes and references

1 M. H. Rashid and T. K. Mandal, *J. Phys. Chem. C*, 2007, **111**, 16750.
2 J. B. Jackson, S. L. Westcott, L. R. Hirsch, J. L. West and N. J. Halas, *Appl. Phys. Lett.*, 2003, **82**, 257.
3 X. Zhou, Y. Zhou, J. C. Ku, C. Zhang and C. A. Mirkin, *ACS Nano*, 2014, **8**, 1511.
4 D. J. Park, C. Zhang, J. C. Ku, Y. Zhou, G. C. Schatz and C. A. Mirkin, *P. Natl. Acad. Sci. USA*, 2015, **112**, 977.
5 S.-S. Chang, C.-W. Shih, C.-D. Chen, W.-C. Lai and C. R. C. Wang, *Langmuir*, 1999, **15**, 701.
6 S. Chen and Y. Yang, *J. Am. Chem. Soc.*, 2002, **124**, 5280.
7 S. E. Skrabalak, J. Chen, Y. Sun, X. Lu, L. Au, C. M. Cobley and Y. Xia, *Acc. Chem. Res.*, 2008, **41**, 1587.
8 A. Halder and N. Ravishankar, *Adv. Mater.* 2007, **19**, 1854.
9 M. Mo, J. Zeng, X. Liu, W. Yu, S. Zhang and Y. Qian, *Adv. Mater.* 2002, **14**, 1658.
10 J. J. Velazquez-Salazar, R. Esparza, S. J. Mejia-Rosales, R. Estrada-Salas, A. Ponce, F. L. Deepak, C. Castro-Guerrero and M. Jose-Yacaman, *ACS Nano*, 2011, **5**, 6272.
11 Y. Wang, Q. Wang, H. Sun, W. Zhang, G. Chen, Y. Wang, X. Shen, Y. Han, X. Lu and H. Chen, *J. Am. Chem. Soc.*, 2011, **133**, 20060.
12 K.-S. Cho, D. V. Talapin, W. Gaschler and C. B. Murray, *J. Am. Chem. Soc.*, 2005, **127**, 7140.
13 P. X. Gao, Y. Ding, W. Mai, W. L. Hughes, C. Lao and Z. L. Wang, *Science*, 2005, **309**, 1700.
14 J. Gao, C. M. Bender and C. J. Murphy, *Langmuir*, 2003, **19**, 9065.
15 N. R. Jana, L. Gearheart and C. J. Murphy, *J. Phys. Chem. B*, 2001, **105**, 4065.
16 T. K. Sau and C. J. Murphy, *Langmuir*, 2005, **21**, 2923.
17 B. Nikoobakht and M. A. El-Sayed, *Langmuir*, 2001, **17**, 6368.
18 P. S. Mdluli, N. M. Sosibo, N. Revaprasadu, P. Karamanis and J. Leszczynski, *J. Mol. Struct.*, 2009, **935**, 32.
19 A. Kedia and S. K. Panidian, *J. Phys. Chem. C*, 2012, **116**, 23721.
20 B. Lim, P. H. C. Camargo and Y. Xia, *Langmuir*, 2008, **24**, 10437.
21 A. A. Umar, M. Oyama, M. M. Salleh and B. Y. Majlis, *Cryst. Growth Des.* 2009, **9**, 2835.
22 Z. L. Wang, R. P. Gao, B. Nikoobakht and M. A. El-Sayed, *J. Phys. Chem. B*, 2000, **104**, 5417.
23 K. Tasaki, *J. Am. Chem. Soc.*, 1996, **118**, 8459.
24 N. Derkaoui, S. Said, Y. Grohens, R. Olier and M. Privat, *J. Colloid Interface Sci.*, 2007, **305**, 330.
25 L. Yang, X. Jiang, W. Ruan, B. Zhao, W. and J. R. Lombardi, *J. Phys. Chem. C*, 2008, **112**, 20095.
26 M.-H. Wang, J.-W. Hu, Y.-J. Li and E. S. Yeung, *Nanotechnology*, 2010, **21**, 145608.